Supplementary Materials

Pei Liu[1], Qinming Wu[1,2,*], Keping Yan[1,2], Liang Wang[1,2], and Feng-Shou Xiao[1,2,*]

[1]College of Chemical and Biological Engineering, Zhejiang University, Hangzhou 310027, Zhejiang, China.
[2]Shanxi-Zheda Institute of Advanced Materials and Chemical Engineering, Taiyuan, 030032, Shanxi, China.

[*]**Correspondence to:** Dr. Qinming Wu, Prof. Feng-Shou Xiao, College of Chemical and Biological Engineering, Zhejiang University, No. 866 Yuhangtang Road, Hangzhou 310027, Zhejiang, China. E-mail: qinmingwu@zju.edu.cn; fsxiao@zju.edu.cn

1. Experimental Section

1.1 Materials

All the chemicals were analytical grade and used as received. Coal fly ash (CFA) used in the present study was obtained from a power plant in Henan, China, and its chemical composition was presented in **Supplementary Table 1**. Sodium hydroxide (NaOH, AR, 96%, Sinopharm Chemical Reagent Co., Ltd.), ammonium chloride (NH_4Cl, AR, 99.5 %, Sinopharm Chemical Reagent Co., Ltd.), hydrochloric acid (HCl, AR, 36.5 %, Sinopharm Chemical Reagent Co., Ltd.), aluminum sulfate octadecahydrate [$Al_2(SO_4)_3 \cdot 18H_2O$, AR, 99 %, Aladdin Chemistry Co., Ltd.], aluminum nitrate nonahydrate [$Fe(NO_3)_3 \cdot 9H_2O$, AR, 98.5 %, Aladdin Chemistry Co., Ltd.], tetraethoxysilane (TEOS, GC, 99 %, Aladdin Chemistry Co., Ltd.), solid silica (Qingdao Haiyang Chemical Reagent Co., Ltd.), and MOR zeolite (SiO_2/Al_2O_3=24, Tianjin Nankai University Catalyst Co., Ltd.) were employed in this work.

1.2 Characterizations

Powder X-ray diffraction (XRD) patterns were measured with a Rigaku Ultimate VI X-ray diffractometer (40 kV, 40 mA) using CuKα (λ=1.5406 Å) radiation. Scanning electron microscopy (SEM) images were employed with Hitachi SU-1510 electron microscopes. Chemical composition of CFA was analyzed by X-ray fluorescence (XRF) on a Bruker S8 TIGER instrument. Nitrogen adsorption-desorption isotherms were measured with a Micromeritics ASAP 2020M and a Tristar system at 77 K. Argon adsorption-desorption isotherms were evaluated with Micromeritics ASAP 2460 at 87 K. Solid-state ^{27}Al magic angle-spinning (MAS) NMR spectra were performed on a Bruker AVANCE III HD spectrometer. The obtained zeolite composition was determined by inductively coupled plasma optical emission spectrometer (ICP-OES) with a Perkin-Elmer 3300DV emission spectrometer. Diffuse reflectance ultravio-let-visible (UV-vis) spectra were measured using a Perkin-Elmer Lambda 20 spectrometer, and $BaSO_4$ was the internal standard. Electron spin resonance spectra (ESR) was measured at X-band (~9 GHz) using Bruker ESRA-300 series.

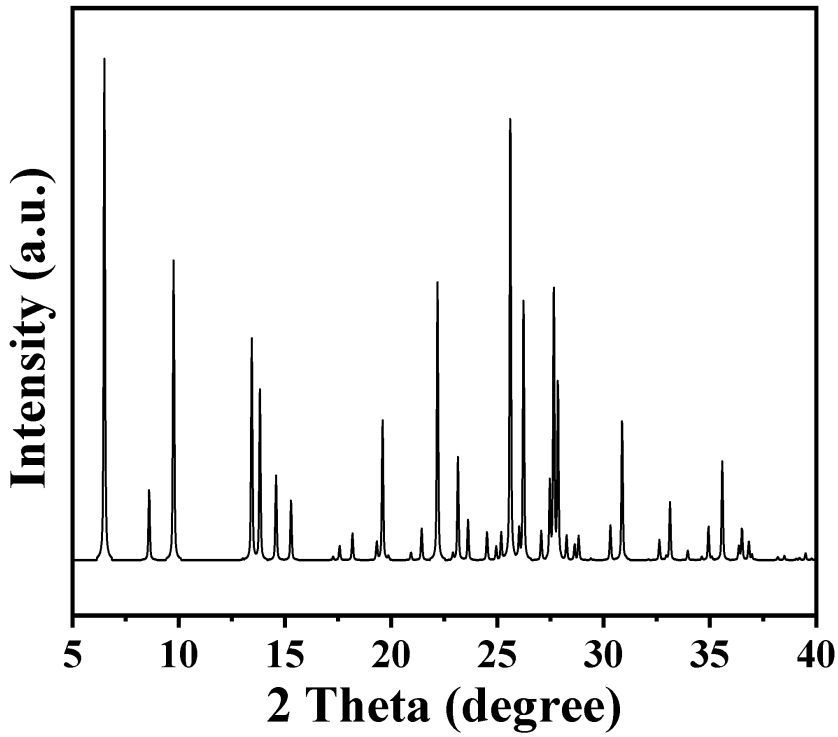

Supplementary Figure 1. The simulated XRD pattern of MOR zeolite structure.

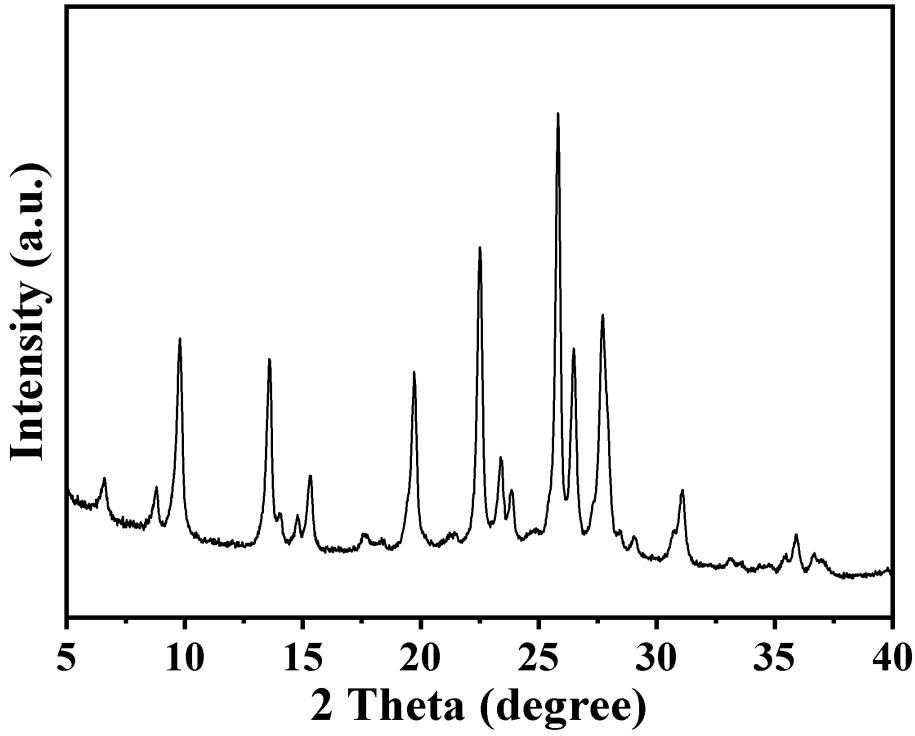

Supplementary Figure 2. XRD pattern of Fe-MOR-ACH zeolite.

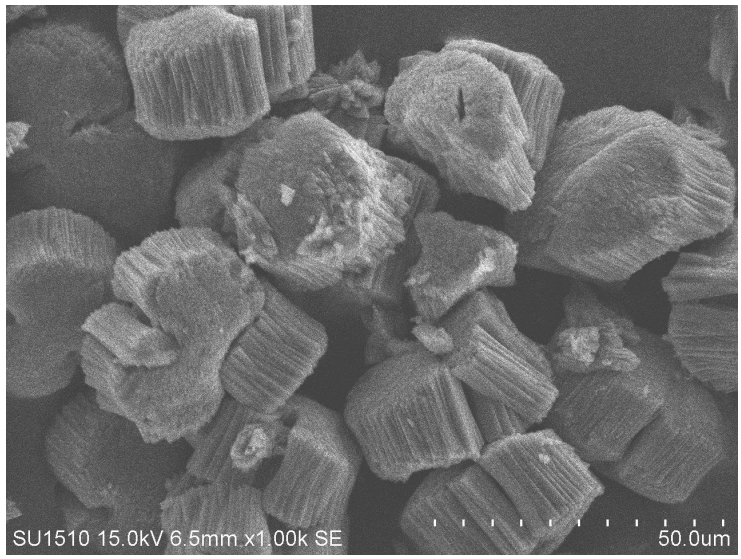

Supplementary Figure 3. SEM image of Fe-MOR-ACH zeolite.

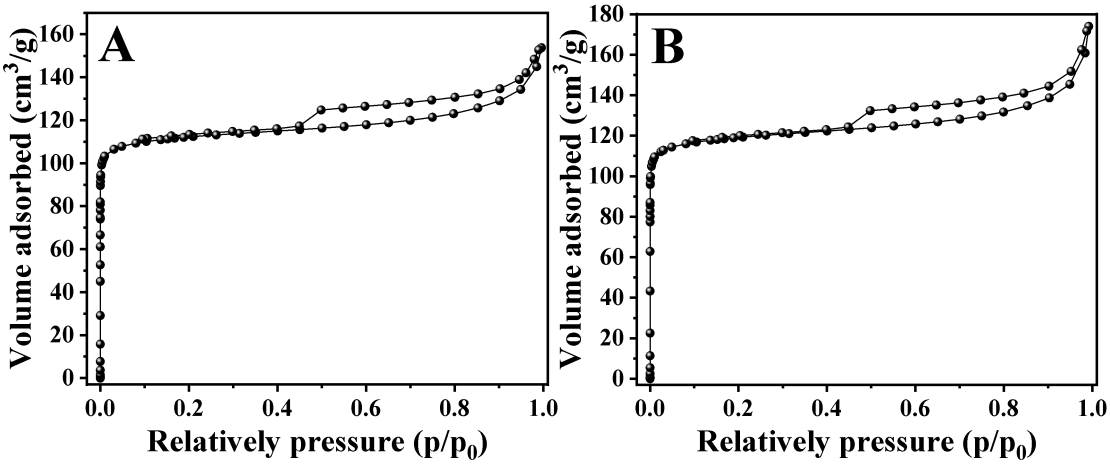

Supplementary Figure 4. N_2 sorption isotherms of (A) conventional MOR zeolite and (B) Fe-MOR-ACH zeolite.

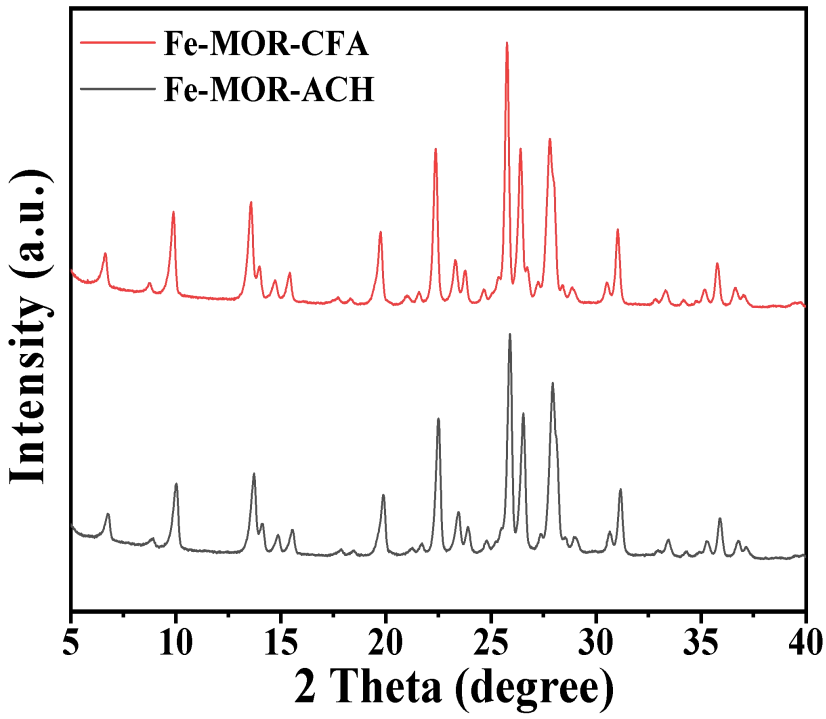

Supplementary Figure 5. XRD patterns of as-calcined Fe-MOR-CFA zeolite and as-calcined Fe-MOR-ACH zeolite.

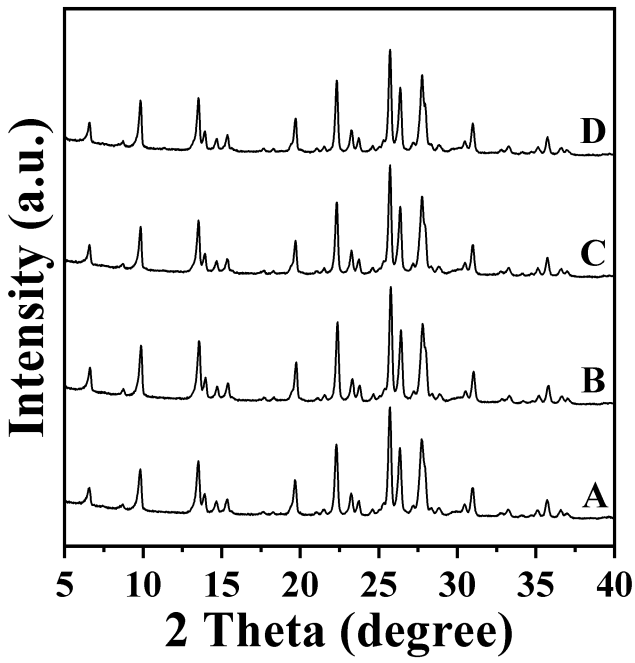

Supplementary Figure 6. XRD patterns of the Fe-MOR-CFA zeolite samples synthesized with the content of zeolite seeds at (A) 0 %, (B) 5 %, (C) 10 %, and (D) 20 %, respectively.

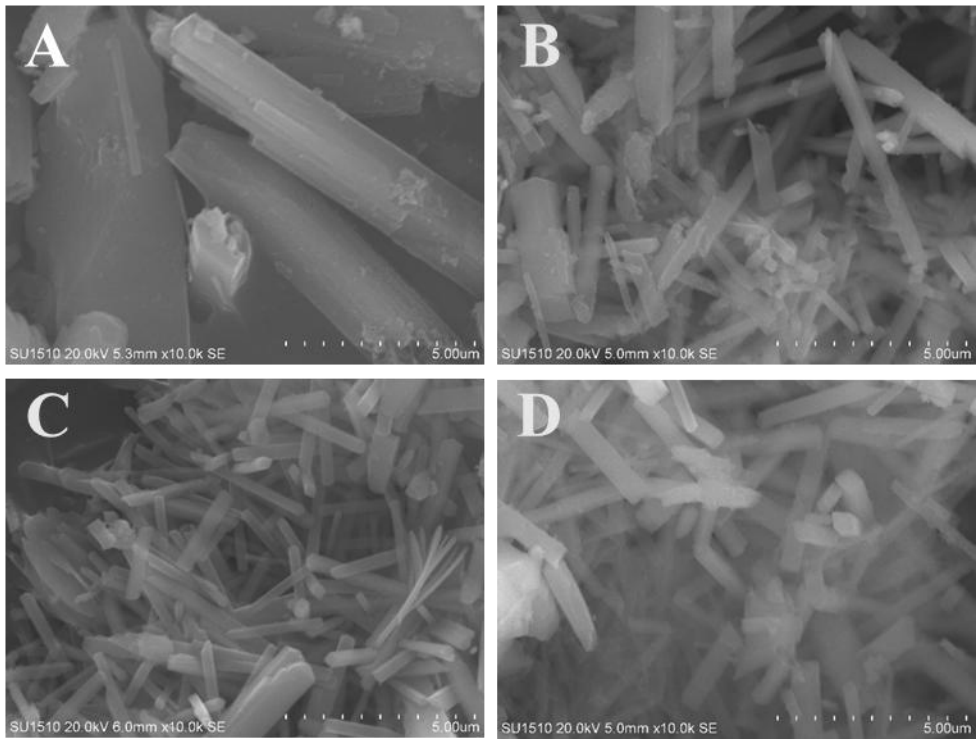

Supplementary Figure 7. SEM images of the Fe-MOR-CFA zeolite samples synthesized with the content of zeolite seeds at (A) 0 %, (B) 5 %, (C) 10 %, and (D) 20 %, respectively.

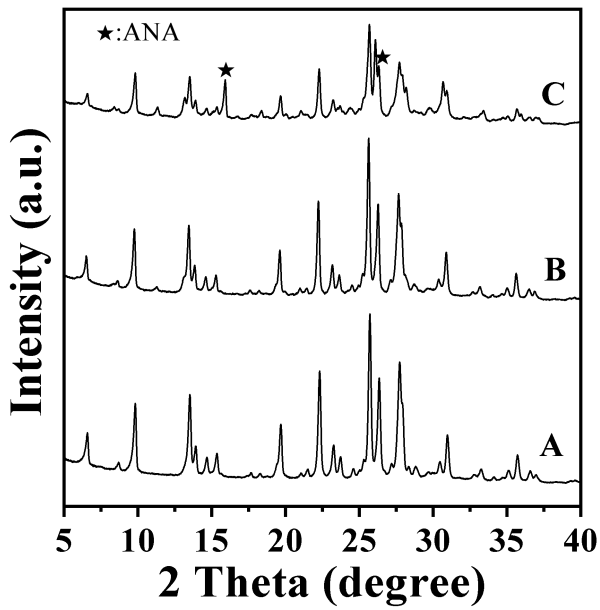

Supplementary Figure 8. XRD patterns of the Fe-MOR-CFA zeolite samples synthesized with the Na_2O/SiO_2 ratios of (A) 0.22, (B) 0.26, and (C) 0.29, respectively.

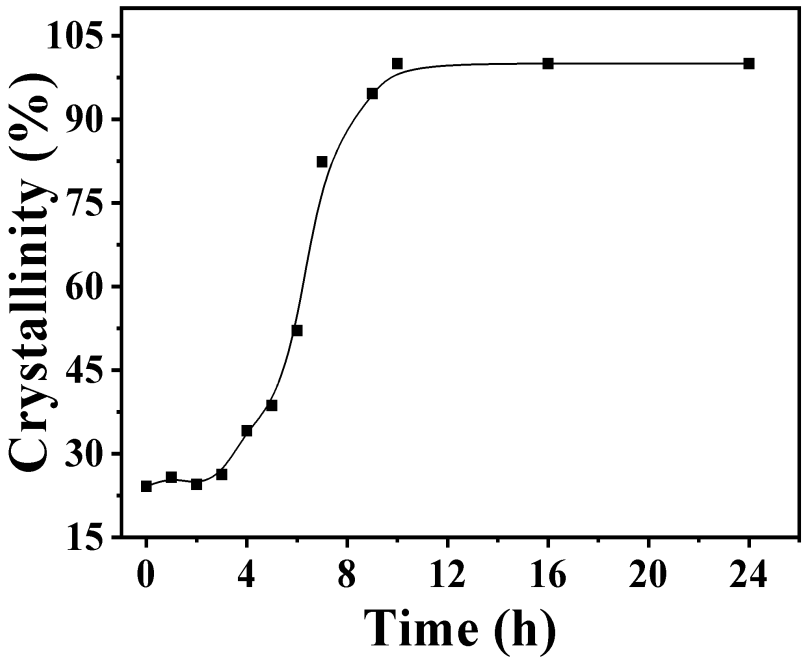

Supplementary Figure 9. The dependence of the Fe-MOR-CFA zeolite crystallinity on crystallization time.

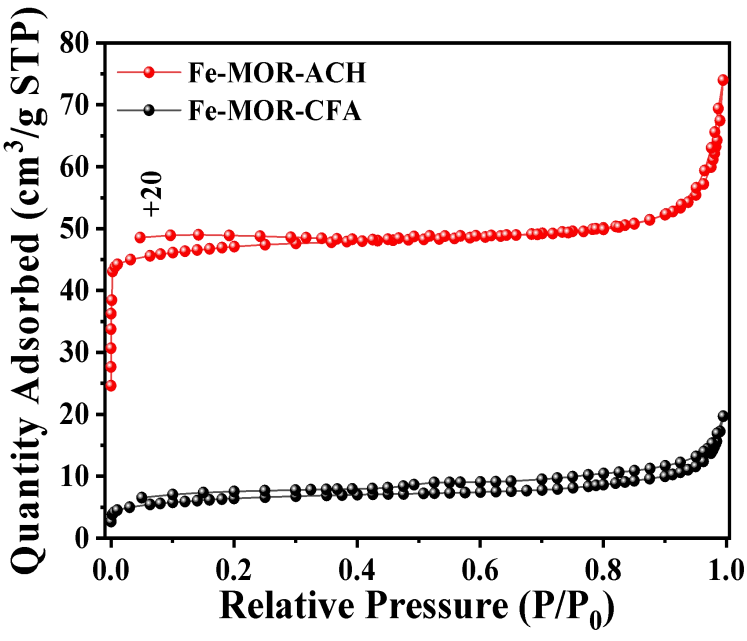

Supplementary Figure 10. N_2 sorption isotherms of Fe-MOR-CFA zeolite and Fe-MOR-ACH zeolite.

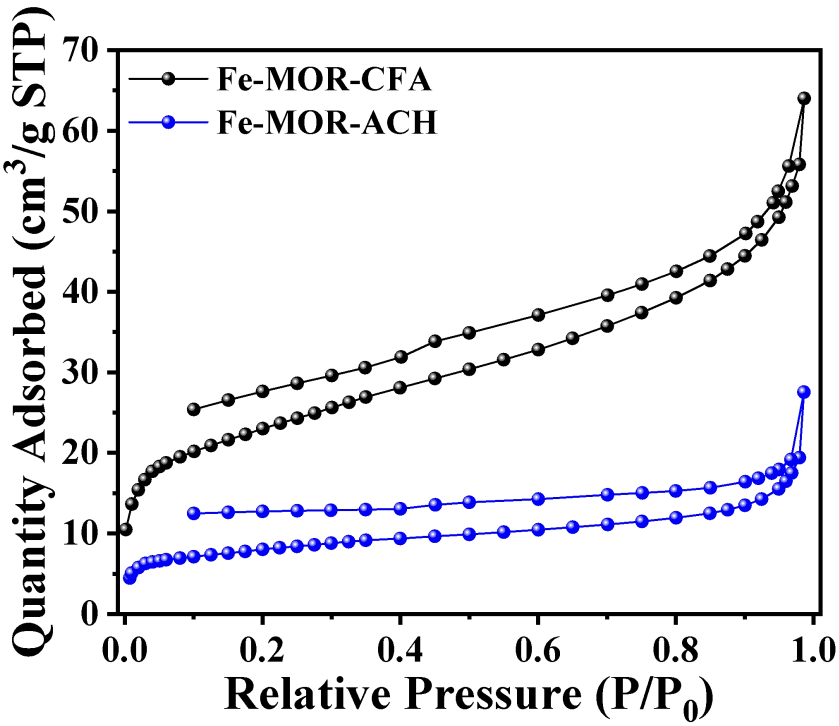

Supplementary Figure 11. Ar sorption isotherms of Fe-MOR-CFA zeolite and Fe-MOR-ACH zeolite.

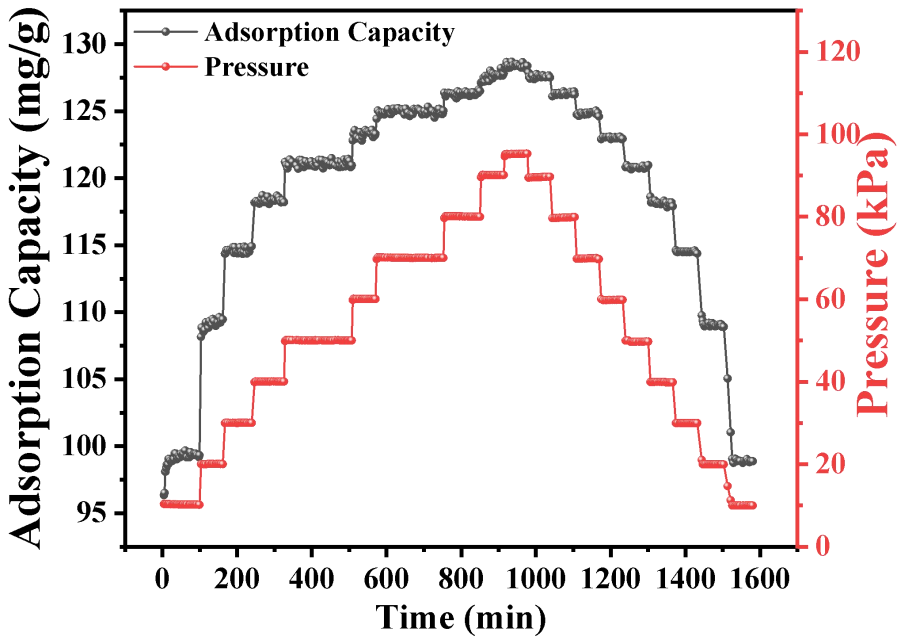

Supplementary Figure 12. Kinetic sorption of CO_2 at 298 K on Fe-MOR-CFA zeolite.

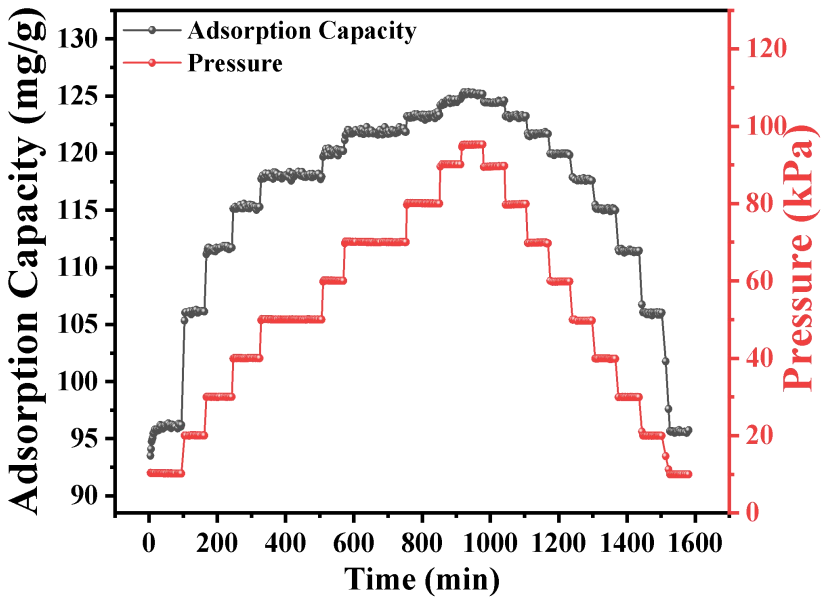

Supplementary Figure 13. Kinetic sorption of CO_2 at 298 K on Fe-MOR-ACH zeolite.

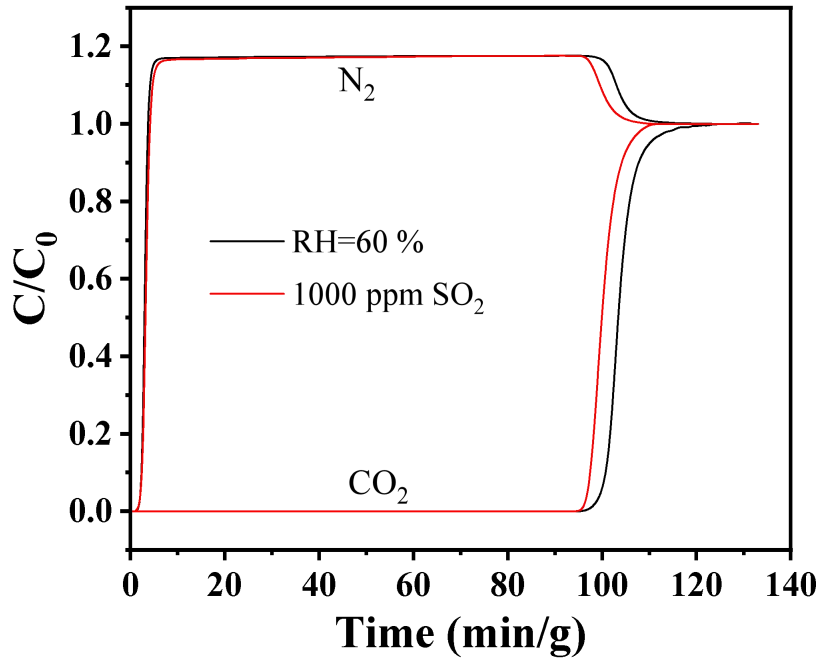

Supplementary Figure 14. Experimental column breakthrough curves over the products with a relative humidity of 60% and the presence of SO_2 (1000 ppm) for the mixture of CO_2/N_2 (15/85, v/v) separation at 298 K.

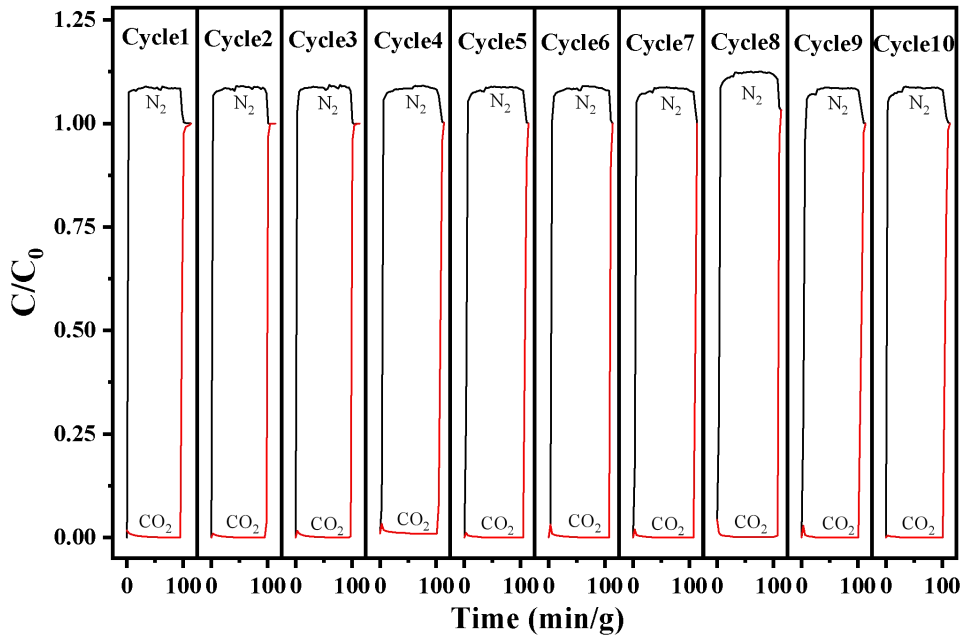

Supplementary Figure 15. Recyclability under CO_2/N_2 (15/85, v/v) column breakthrough tests over the Fe-MOR-CFA zeolite.

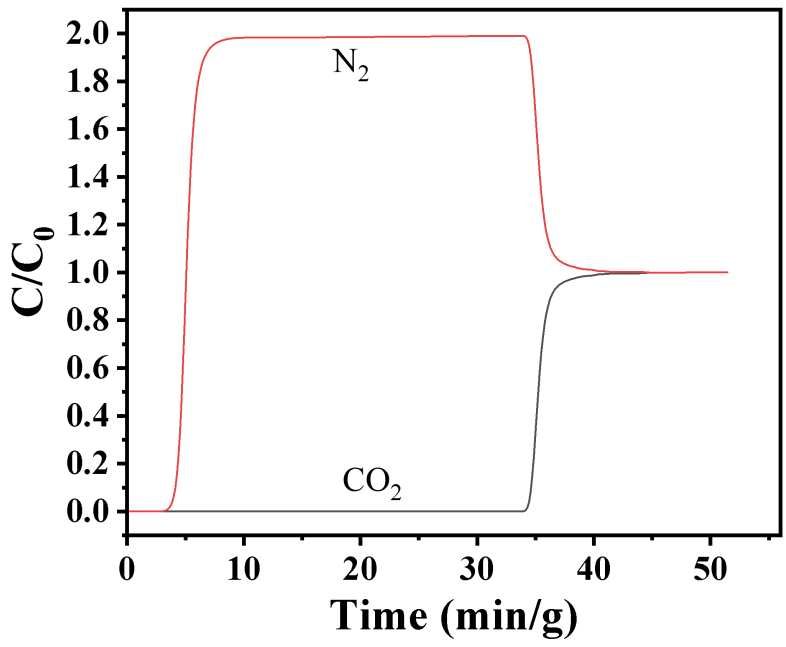

Supplementary Figure 16. Experimental column breakthrough curves for the mixture of CO_2/N_2 (50/50, v/v) separation over Fe-MOR-CFA zeolite at 298 K.

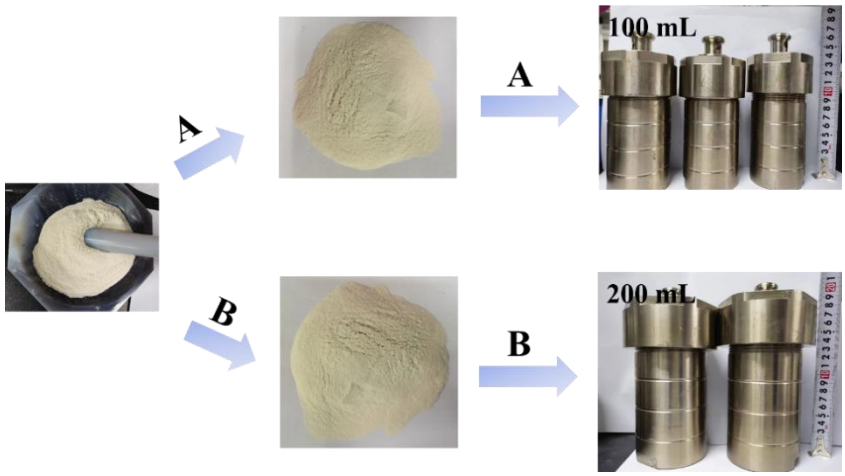

Supplementary Figure 17. Photographs of the Fe-MOR-CFA zeolite synthesized in the scale of (A) 100 mL and (B) 200 mL.

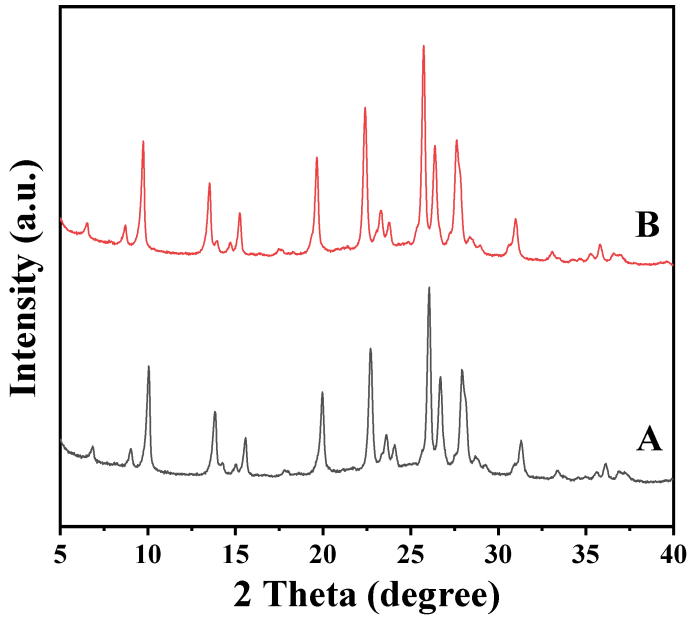

Supplementary Figure 18. XRD patterns of the Fe-MOR-CFA zeolite synthesized in the scale of (A) 100 mL and (B) 200 mL.

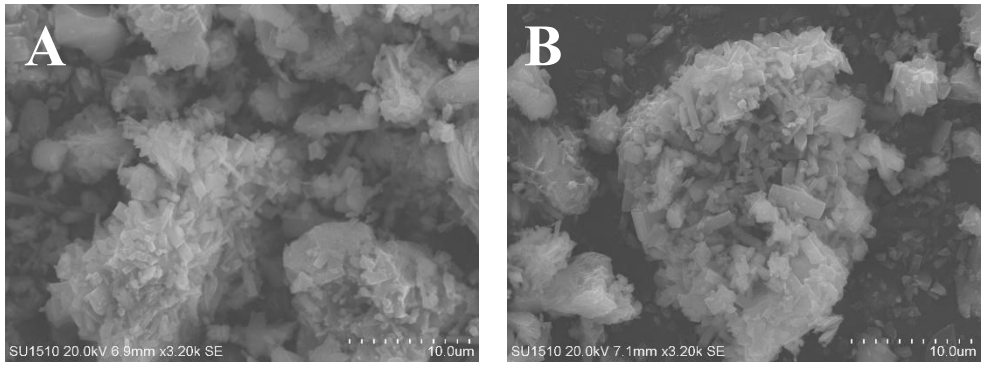

Supplementary Figure 19. SEM images of the Fe-MOR-CFA zeolite synthesized in the scale of (A) 100 mL and (B) 200 mL.

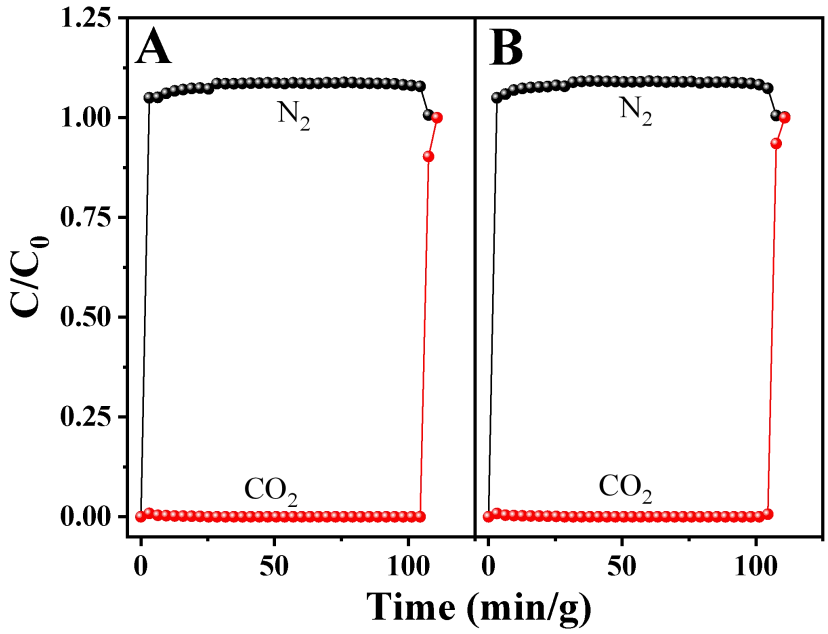

Supplementary Figure 20. The column breakthrough curves of the Fe-MOR-CFA zeolite for the mixture of CO_2/N_2 (15/85, v/v) at 298 K synthesized in the scale of (A) 100 mL and (B) 200 mL.

Supplementary Table 1. Chemical compositions of the samples measured by XRF

Sample	Chemical composition (wt.%)									
	SiO_2	Al_2O_3	Fe_2O_3	Na_2O	CaO	K_2O	TiO_2	SO_3	Loss of ignition (Ig)	other
CFA	52.00	29.20	3.33	-	2.00	1.46	1.19	0.63	9.04	1.15
CFA-NaOH	27.60	14.70	3.01	43.70	0.92	0.87	0.55	0.33	8.90	0.98
Fe-MOR-CFA	78.29	9.50	2.10	8.24	0.50	0.46	0.34	-	-	0.57

Supplementary Table 2. Textural parameters of Fe-MOR-CFA zeolite and Fe-MOR-ACH zeolite measured with N_2 and Ar sorption isotherms

Sample	Adsorbate	$S_{BET}(m^2/g)$	$V_{total}(cm^3/g)$	$V_{micro}(cm^3/g)$
Fe-MOR-CFA	N_2	22	0.02	0.01
Fe-MOR-ACH	N_2	28	0.02	0.02
Fe-MOR-CFA	Ar	72	0.08	0.02
Fe-MOR-ACH	Ar	25	0.04	0.01

Supplementary Table 3. Reproducible CO_2/N_2 (15/85, v/v) separation performance of Fe-MOR-CFA zeolite at 298 K

Cycle times	CO_2 retaining time (min/g)	CO_2 uptake (mmol/g)
1	95.3	1.92
2	96.3	1.93
3	98.3	1.97
4	99.1	1.99
5	98.6	1.98
6	104.7	2.10
7	103.9	2.09
8	102.7	2.06
9	101.2	2.03
10	100.6	2.02